

Status of the ATLAS Tile Calorimeter

Henric Wilkens^{1,*}, on behalf of the ATLAS collaboration

¹CERN

Abstract. The Tile Calorimeter (TileCal) is a sampling hadronic calorimeter covering the central region of the ATLAS experiment, with steel as absorber and plastic scintillators as active medium. The scintillators are read-out by the wavelength shifting fibres coupled to the photomultiplier tubes (PMTs). The analogue signals from the PMTs are amplified, shaped, digitised by sampling the signal every 25 ns and stored on detector until a trigger decision is received. The TileCal front-end electronics reads out the signals produced by about 10000 channels measuring energies ranging from about 30 MeV to about 2 TeV. Each stage of the signal production from scintillation light to the signal reconstruction is monitored and calibrated. A summary of recent performance results and its High Luminosity LHC upgrade project will be presented.

1 Introduction

TileCal is the central part of the ATLAS hadronic calorimeters, and covers pseudo-rapidities up to 1.7, and has a depth of 7 interaction lengths. It consists of three steel absorber structures, barrels, each built of 64 modules, in which scintillating tiles are inserted. The central barrel is called Long Barrel (LB) and contains the LAr barrel electromagnetic calorimeter and the inner tracker, and is flanked on each side with a barrel called Extended Barrel (EB), containing the LAr electromagnetic and hadronic End Cap detectors as well as the forward calorimeters. Each tile is coupled to two PMTs (Hamamatsu R7877) by means of wavelength shifting fibres (Kuraray Y11(200)MSJ). Multiple tiles are read by the same pair of PMTs, and define cells, allowing segmentation in η , ϕ and 3 radial layers. These proceedings will present selection of the results from the TileCal collaboration, from LHC Run-3 for the calibration systems, from Run-2 for performance studies. It will discuss the calorimeter's High Luminosity LHC (HL-LHC) upgrade program, and finish with the activities at the CERN SPS test-beams.

2 Calibration of the Tile Calorimeter

The response of the calorimeter evolves over time, due to effects such as the degradation of the optical properties of the scintillators and wavelength shifting fibres, or gain change of the PMT when under stress. A series of calibration systems allow to monitor and correct for the response evolution. The energy deposited in a cell is estimated from the digitised PMT using the formula in Equation 1. The amplitude is obtained through optimal filtering of the digi-

tised ADC readings.

$$E_{\text{pmt}} = \text{Amplitude} \times C_{\text{ADC} \rightarrow \text{pC}} \times \xi_{\text{laser}} \times \xi_{\text{Cs}} \times C_{\text{pC} \rightarrow \text{MeV}} \quad (1)$$

A charge injection system into the fast ADC allows to obtain the $C_{\text{ADC} \rightarrow \text{pC}}$ factor. A laser system injects short light pulses into the PMTs and is readout by the fast ADC, and allows to extract the factor ξ_{laser} . A hydraulic system drives a small capsule loaded with ^{137}Cs through any tile in the calorimeter and the PMT currents readout by a slow ADC allows to extract the ξ_{Cs} factor. Finally the $C_{\text{pC} \rightarrow \text{MeV}}$ factor has been obtained from the beam test of 11% of the modules at the SPS H8 line before installation in the ATLAS experiment.

2.1 Cesium calibration

The cesium calibration system [1] uses a 4.3 km hydraulic circuit in the LB (2.4 km in each EB) to drive a radioactive capsule through each tile. The three sources (one per barrel) had an activity of order 370 MBq in 2009. The photons from the ^{137}Cs decays induce scintillation light in the tiles, which is collected by the wavelength shifting fibres and channeled to the PMTs which are readout by a slow ADC after signal integration, through a low pass filter with a time constant of order 10 ms. A dedicated charge injection system allow to calibrate the integrator readout system. As the scan with the radioactive source takes several hours, they are performed during longer stops of the LHC accelerator, with a periodicity of one month.

Figure 1 shows the evolution of the average response variation for each radial layer of the extended barrels during the first two years of LHC Run-3, and compares it to the LHC delivered luminosity in gray. The evolution is driven by two main factors: the radiation induced ageing of the optical components and the short time PMT gain variations due to the currents traversing them. The latter

*e-mail: Henric.Wilkens@cern.ch

© Copyright CERN for the benefit of the ATLAS Collaboration. CC-BY-4.0 license

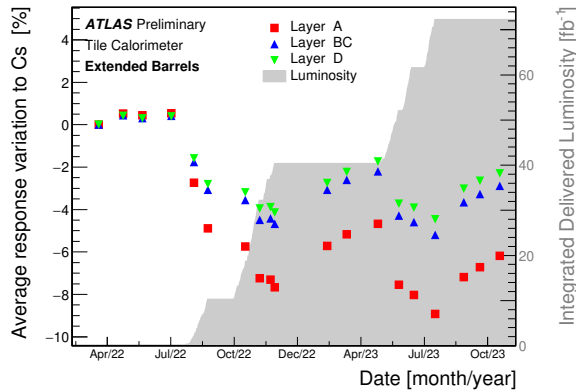


Figure 1. Average relative response variation of TileCal cells in Extended Barrels to cesium source as a function of time in 3 different longitudinal layers during Run-3

component is responsible for the fast drop when LHC resumes collisions and the slow recovery, in the time scale of weeks, when LHC is in maintenance. The radiation damage is to a large extent not recoverable. The integrator readout is also operated during physics runs, collecting the charges induced by the particle from Minimum Bias collisions, for luminosity measurements and cross calibration studies.

2.2 Charge injection calibration

For the fast readout of the PMTs, the signal of each PMT is shaped and amplified with two different gains, with a ratio of 1 to 64, and digitised by ADCs, one for each gain. A dedicated set of capacitors, charged by a DAC is used to inject well defined charges at a controllable phase with respect to the sampling 40 MHz clock. Every second day a set of dedicated runs are collected in between LHC fills, allowing to extract the ADC to charge calibration factors. Given the very good stability of the coefficient over time, they are updated monthly for use by the ATLAS offline reconstruction.

2.3 Laser calibration

The laser calibration system [2] delivers short (10 ns) pulses at 532 nm wavelength, from a laser (Spectra Physics model J40-BLS6), to each PMT, and a set of photodiodes used to normalise the laser signals. The laser calibration data is collected in dedicated runs, every second day, in between LHC fills, at two different intensities. The two different intensities are chosen as to be in the range of the high and low gain ADCs. The data collected allows for weekly updates of the laser calibration factors. Figure 2 shows the evolution of the average gain variation as a function of time for the first two years of operation of LHC Run-3. Contrary to the cesium system, the laser system is not sensitive to the radiations induced aging of the scintillators and wavelength shifting fibres. The laser system is also used during physics runs, pulsing during the

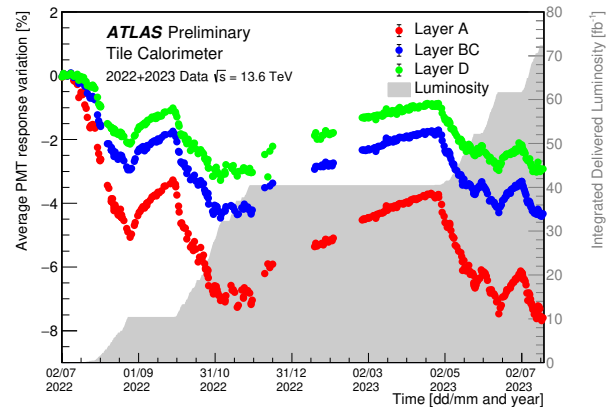


Figure 2. Average relative gain variation as a function of time in three different longitudinal layers during Run-3

abort gap, a period without collisions in the LHC orbit. This data is used to derive timing corrections.

3 Ageing studies

The cesium calibration system and Minimum Bias (MB) currents readout are sensitive to both scintillator ageing and PMT gain variations, while the laser is only sensitive to the latter. This allows to extract the degradation of the optical instrumentation of the calorimeter through Equation 2.

$$I/I_0 = \frac{\Delta R_{Cs/MB}}{\Delta R_{Las}} = p_0 e^{-dose/p_1} \quad (2)$$

Figure 3 shows the average light yield measurements for the most exposed cell, A13, in the calorimeter. The fitted function to the cesium and MB data is extrapolated to the expected dose at the end of LHC (corresponding to an integrated luminosity of 450 fb^{-1}) and the end of HL-LHC (corresponding to 4000 fb^{-1}). It also shows the result obtained on the bare scintillators obtained a month after the irradiation tests done at construction time, at a much higher dose rate. Studies by the CMS experiment [4] show a strong dependence on the degradation rate parameter p_1 as function of the dose rate, with smaller dose rates leading to higher degradation rates. TileCal data suggests the same dependence. This would result in a smaller degradation by the end of HL-LHC, due to higher dose rate, indicated by the orange band in Figure 3. A dedicated publication is in preparation.

4 Performance studies

In this section, the quality to the energy reconstruction in the calorimeter is going to be tested by comparing the reconstructed energy of particles from collision, with Monte-Carlo (MC) simulations. Data collected during LHC run-2, after reprocessing with the final calibration constants is used. The full set of results from Run-2 are available in Ref. [3].

Table 1. The response ratio R_i of the cells of different radial layers in the LB and EB obtained by analysing 2015–2016, 2017 and 2018 data. Statistical (first value) and systematic (second value) uncertainties are shown.

Layer	$R_i(2015 - 2016)$	$R_i(2017)$	$R_i(2018)$
LB-A	$0.988 \pm 0.001 \pm 0.003$	$0.996 \pm 0.002 \pm 0.007$	$0.996 \pm 0.001 \pm 0.004$
LB-BC	$0.984 \pm 0.001 \pm 0.001$	$0.993 \pm 0.001 \pm 0.002$	$0.992 \pm 0.001 \pm 0.003$
LB-D	$1.014 \pm 0.001 \pm 0.004$	$1.019 \pm 0.001 \pm 0.003$	$1.024 \pm 0.001 \pm 0.002$
EB-A	$1.006 \pm 0.003 \pm 0.006$	$1.029 \pm 0.002 \pm 0.006$	$1.016 \pm 0.002 \pm 0.006$
EB-B	$0.978 \pm 0.002 \pm 0.002$	$0.990 \pm 0.001 \pm 0.006$	$0.989 \pm 0.001 \pm 0.004$
EB-D	$0.982 \pm 0.001 \pm 0.004$	$0.990 \pm 0.001 \pm 0.007$	$0.997 \pm 0.001 \pm 0.004$

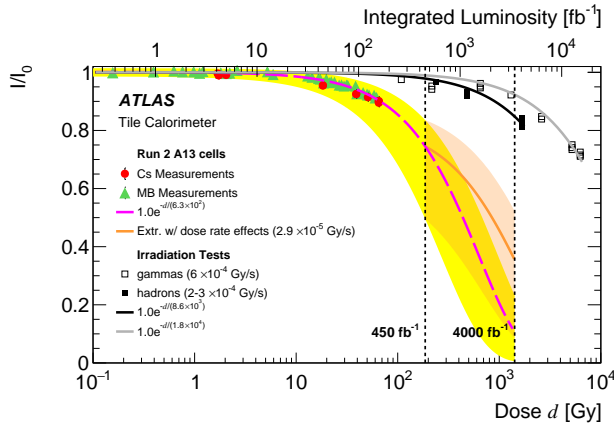


Figure 3. Average relative light yield (I/I_0) measurements based on the cesium system (dots) and integrated minimum-bias currents (triangles) for A13 cells as a function of average simulated dose d and LHC integrated luminosity.

4.1 Muons from collision

High energy muons, obtained in significant amounts from $W \rightarrow \mu\nu$ decays are standard candles which can be used to validate the calorimeter energy reconstruction at low energies. Muons deposit by ionisation typically a few hundred MeV to couple of GeV in TileCal cells, depending on the path length of the trajectory through the cell. For each cell traversed by the muon, the energy loss $\frac{\Delta E}{\Delta x}$ is calculated. Then the ratio R of the average energy loss for data to the average for MC is obtained. Table 1 shows the resulting mean R_i per layer in depth, for three periods during Run-2. In each period the standard deviation of the distributions of the measurements listed in the Table is 1.5%.

4.2 Isolated hadrons

The calorimeter energy response is probed by measuring the energy deposited in the calorimeter by isolated hadrons produced in the pp collisions. The determination is obtained using the ratio E/p , where E is the energy measured by the calorimeters and p the momentum measured by the inner detector. The particles have a momentum below 20 GeV and the precision of the measurement is dominated by the energy resolution. Each event is required to have a well reconstructed vertex with at least four well reconstructed associated tracks with $p_T > 400$ MeV. Each track selected for this study is required to have

$p_T > 500$ MeV and $|\eta| < 2.5$. To select isolated single charged hadrons, no other track is allowed within a cone of $\sqrt{(\Delta\eta)^2 + (\Delta\phi)^2} < 0.4$ centred on the considered track. Muon and neutrals are removed from the analysis, and the energy deposited in the electromagnetic calorimeter is required to be compatible with a minimum ionising particle.

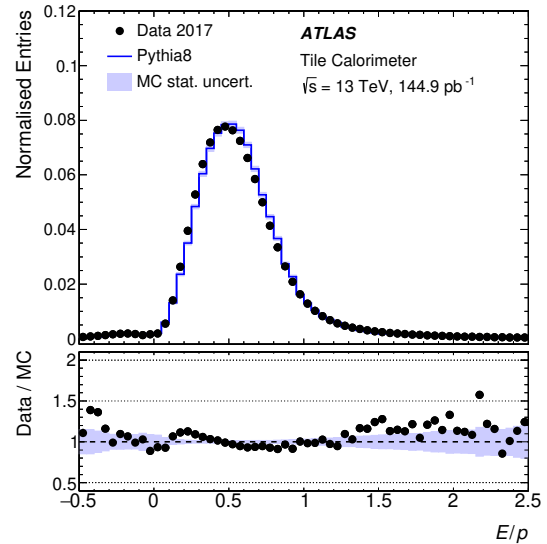


Figure 4. The distribution of the ratio of the energy of isolated hadrons measured by the calorimeters divided by the momentum of the track measured by the inner detector (E/p). The distribution obtained by analysing simulated data is also shown. The distributions are normalised to an integrated area of one. The ratios of the experimental values to the simulated ones are plotted in the lower panel. The MC statistical uncertainties are shown.

The E/p distribution is shown in Figure 4. Due to the non-compensating nature of the calorimeter, and a mean E/p of 0.5896 ± 0.0001 is obtained (0.593 ± 0.001 for simulations). Only statistical uncertainties are quoted. The comparison between the results obtained by analysing experimental and simulated data shows a good reconstruction of the energy at the electromagnetic scale of low momentum hadrons with an uncertainty better than 5%. See Table 2.

5 The upgrade for HL-LHC

The HL-LHC era will bring new challenges in term of instantaneous luminosity, five times higher, higher pile-up

Table 2. Ratios of the $\langle E/p \rangle$ values obtained from experimental and simulated data. The results were obtained by analysing isolated hadrons with different pseudo-rapidity and momentum values. Statistical and systematic uncertainties are combined in quadrature.

	$ \eta < 0.7$	$0.7 \leq \eta \leq 1.0$	$1.0 < \eta \leq 1.7$
$2.0 \text{ GeV} \leq p < 3.0 \text{ GeV}$	0.98 ± 0.01	0.97 ± 0.01	1.03 ± 0.05
$3.0 \text{ GeV} \leq p < 4.0 \text{ GeV}$	0.98 ± 0.01	0.97 ± 0.01	1.00 ± 0.03
$4.0 \text{ GeV} \leq p < 5.0 \text{ GeV}$	0.97 ± 0.02	0.98 ± 0.02	0.99 ± 0.02
$5.0 \text{ GeV} \leq p < 7.0 \text{ GeV}$	0.98 ± 0.01	0.96 ± 0.02	0.97 ± 0.02
$p \geq 7.0 \text{ GeV}$	1.01 ± 0.03	1.02 ± 0.05	0.98 ± 0.02

and radiation environment. It will require high frequency trigger readout. To cope with its extended lifetime, TileCal will undergo an extensive upgrade [5]. Its on- and off-detector electronics will be fully replaced, providing a 40 MHz continuous data readout of all channels, and delivery of trigger primitives at this frequency. The throughput will reach 40 Tb/s over 6000 optical links. The radiation hardness of the on-detector electronics will be improved, as well as its reliability. New mechanical supports have been produced with improved maintainability by a more modular design. About 10% of the PMTs will be replaced with more stable Hamamatsu R11187 PMTs. New high and low voltage supplies will provide the necessary power with an improved granularity.

6 Testbeam campaigns

The TileCal collaboration is conducting yearly testbeam campaigns at CERN's SPS H8 beamline since 2015, with two LB modules and an EB module, equipped with legacy and upgraded electronics to validate the design choices made for the electronics and to study the physics of calorimetry in cooperation with the GEANT4 team. Electron, muon and hadron beams of various energies have been used on different detector orientations. The beam line is equipped with Cherenkov detectors allowing for particle identification. Results were published in Ref. [6]. A notable result is the comparative calorimeter response, to pions, kaons and protons in the energy range of 16 to 30 GeV.

7 Conclusions

The ATLAS Tile Calorimeter continues to operate well through the LHC Run-3 with results from the calibration systems according to our expectations. Extensive studies of the data collected during Run-2 have been performed. Further studies of the calorimeter ageing are on-going, but give confidence for the HL-LHC era, with a dedicated

publication in preparation. Results from muons and single hadron responses show good agreement with simulations. The full set of results from Run-2 is available in Ref. [3]. The HL-LHC era will extend the lifetime of the detector by decades, and present many challenges. For this, an extensive upgrade project will replace all on- and off-detector electronics, and about 10% of the PMTs. Yearly test-beam campaigns since 2015 allow to validate design choices made in the prototypes for the upgrade project, as well as to study the physics of hadronic calorimetry.

References

- [1] G. Blanchot *et al*, The Cesium source calibration and monitoring system of the ATLAS Tile Calorimeter: design, construction and results. JINST **15**, P03017 (2020). <https://dx.doi.org/10.1088/1748-0221/15/03/P03017>
- [2] M.N. Agaras *et al*, Laser calibration of the ATLAS Tile Calorimeter during LHC Run-2. JINST **18**, P06023 (2023). <https://dx.doi.org/10.1088/1748-0221/18/06/P06023>
- [3] The ATLAS collaboration, Operation and Performance of the ATLAS tile calorimeter in LHC Run-2. Accepted for publication by Eur. Phys. J. C <https://arxiv.org/abs/2401.16034>
- [4] V. Khachatryan *et al.*, Dose rate effects in the radiation damage of the plastic scintillators of the CMS hadron endcap calorimeter. JINST **11**, T10004 (2016). <https://dx.doi.org/10.1088/1748-0221/11/10/T10004>
- [5] ATLAS Collaboration, Technical Design Report for the Phase-II Upgrade of the ATLAS Tile Calorimeter. CERN-LHCC-2017-019, (2017). <https://cds.cern.ch/record/2285583>
- [6] J. Abdallah *et al*, Study of energy response and resolution of the ATLAS Tile Calorimeter to hadrons of energies from 16 to 30 GeV, Eur. Phys. J. C **81** (2021), 549. <https://link.springer.com/article/10.1140/epjc/s10052-021-09292-5>